

ESI

Wafer-sized 2D Perovskite Single Crystal Thin Film for UV Photodetector

*Sheng Wang,^{ab} Yuan Chen,^{*b} Junjie Yao,^b Guoxiang Zhao,^b Longzhi Li,^{*a} Guifu
Zou^{*ab}*

^a College of Mechanical and Electronic Engineering, Shandong University of
Science and Technology, Qingdao, 266590, P.R. China.

^b College of Energy, Soochow Institute for Energy and Materials Innovations,
and Key Laboratory of Advanced Carbon Material and Wearable Energy
Technologies of Jiangsu Province, Soochow University, Suzhou, 215006, P.R.
China.

*Correspondence and requests for materials should be addressed to:

Y. Chen: email: ychen216@stu.suda.edu.cn

L.Z. Li: email: lilongzhi630@163.com

G.F. Zou: email: zouguifu@suda.edu.cn



Fig. S1 Schematic illustration of the growth of BA_2PbBr_4 single crystal thin films by a gas-liquid interface crystalline route.

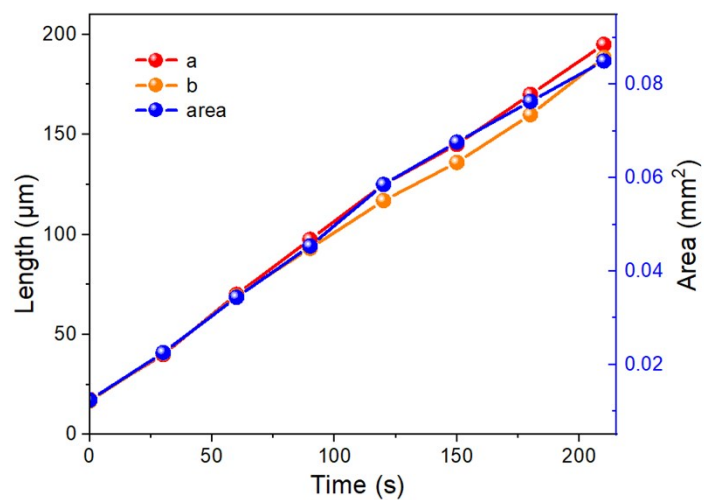


Fig. S2 The length and area of the BA_2PbBr_4 SCTF change with time.

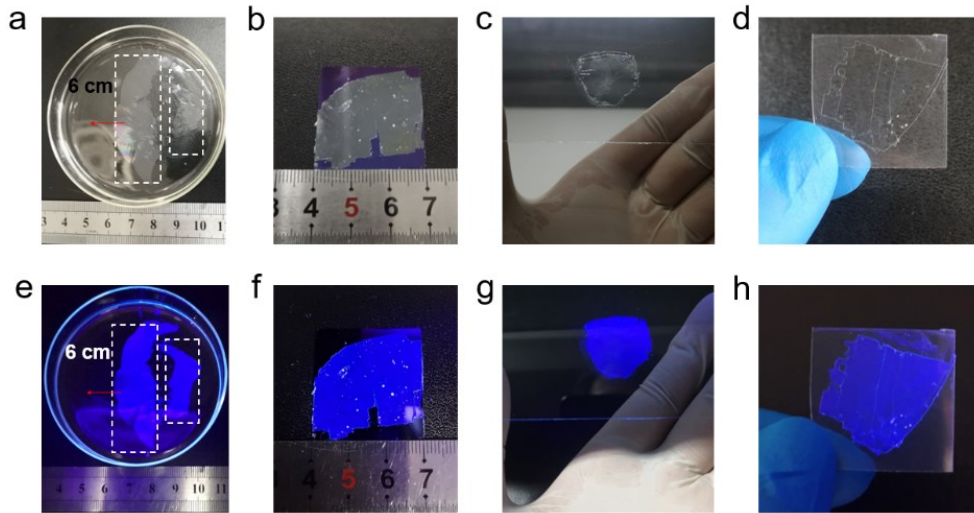


Fig. S3 Photographs of the BA_2PbBr_4 SCTF. (a) BA_2PbBr_4 SCTF in solution (b) transferred on SiO_2 (c) glass (d) PET. (e-f) Photographs corresponding to the above one by one under strong UV lamp, the excitation wavelength is 375 nm.

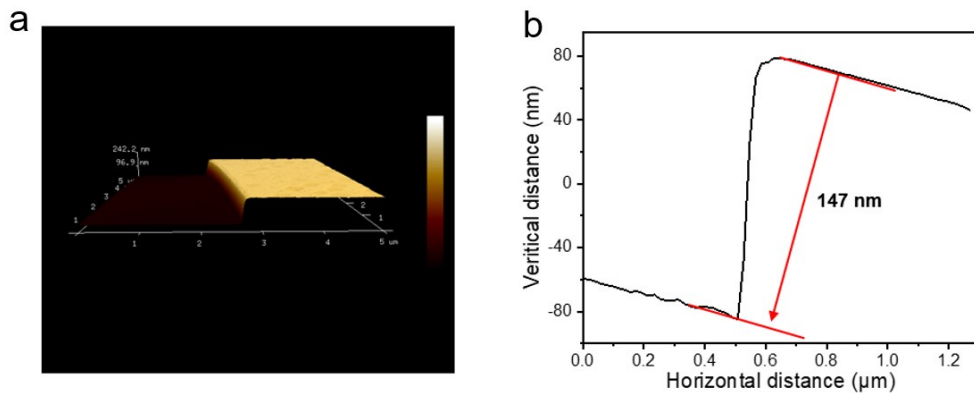


Fig. S4 (a) 3D AFM topographic of a BA_2PbBr_4 SCTF. (b) Height profile of the line scan.

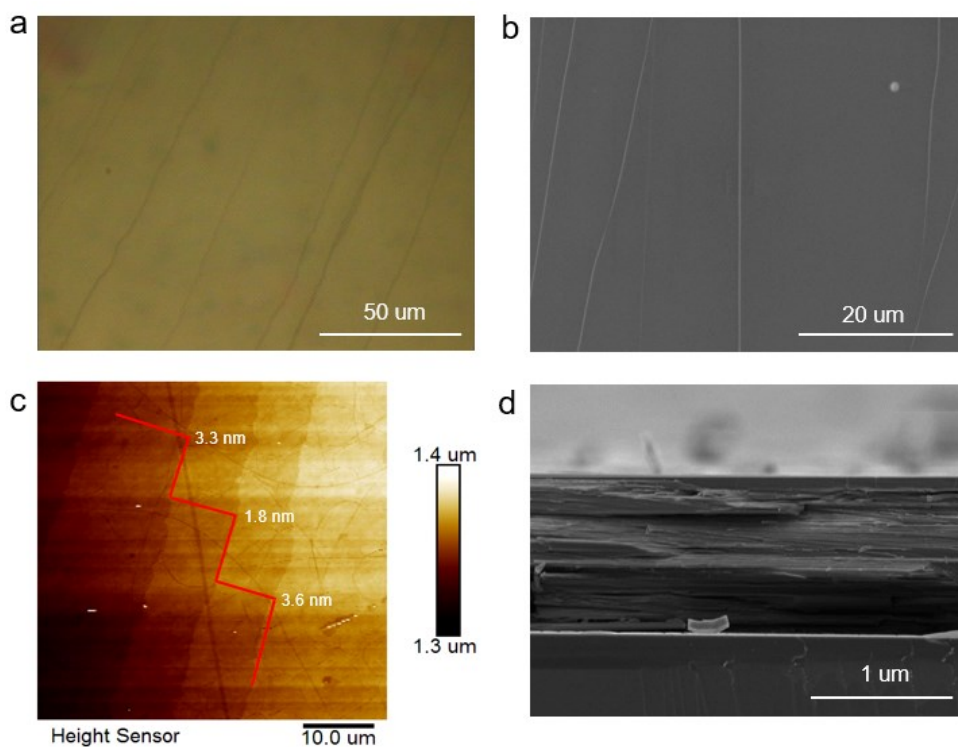


Fig. S5 (a) Optical image of the BA_2PbBr_4 crystalline surface. (b) SEM image of the BA_2PbBr_4 crystalline top view. (c) AFM image of a BA_2PbBr_4 crystalline surface. (d) Cross-sectional SEM image of layered BA_2PbBr_4 crystal.

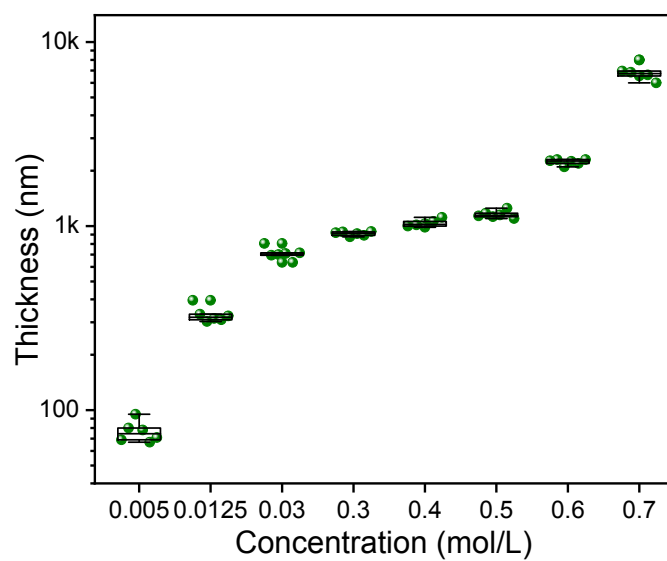


Fig. S6 Statistics of film thickness under different concentrations.

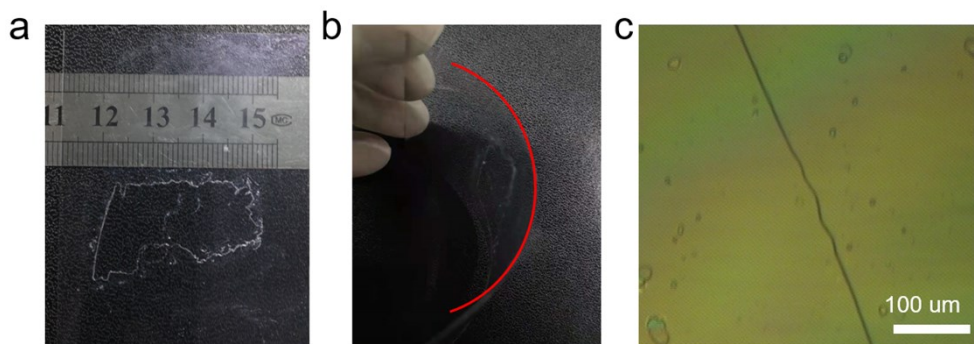


Fig. S7 (a) A complete BA_2PbBr_4 SCTF transferred to PET substrates. (b) The photograph showing the flexing angle for the BA_2PbBr_4 SCTF. (c) Photograph of the BA_2PbBr_4 SCTF after bending.

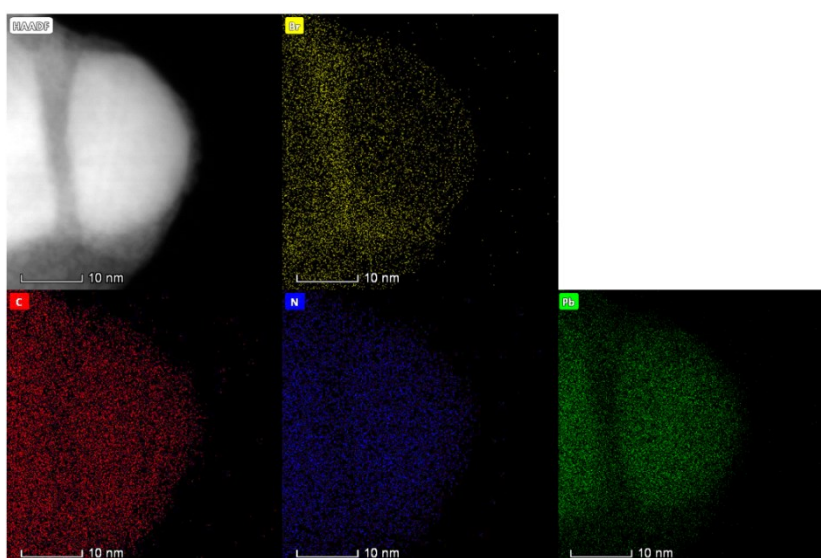


Fig. S8 HAADF imaging and corresponding STEM-EDS elemental mapping of Br, C, N and Pb, respectively.

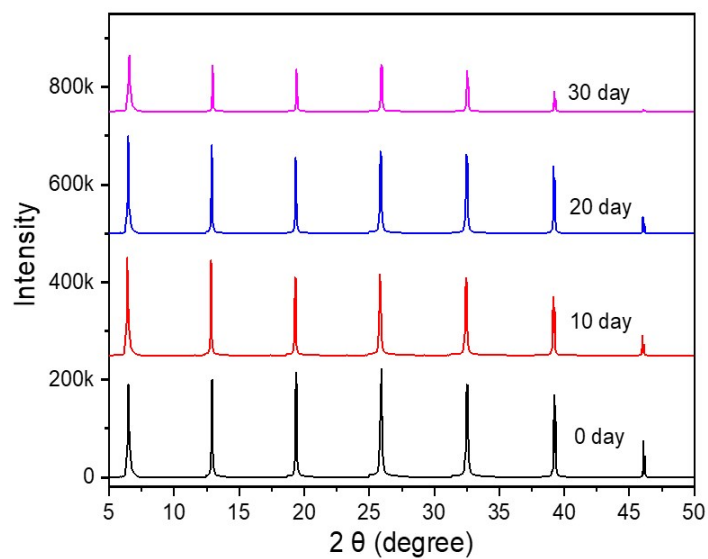


Fig. S9 XRD patterns of BA_2PbBr_4 perovskite stored for 30 days under ambient environment.

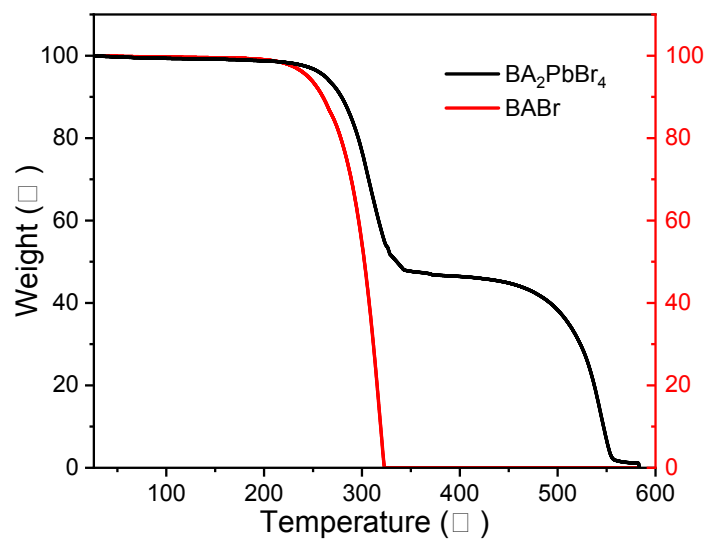


Fig. S10 The thermal stability of the BA_2PbBr_4 and BAbR crystal powder measured using thermogravimetric.

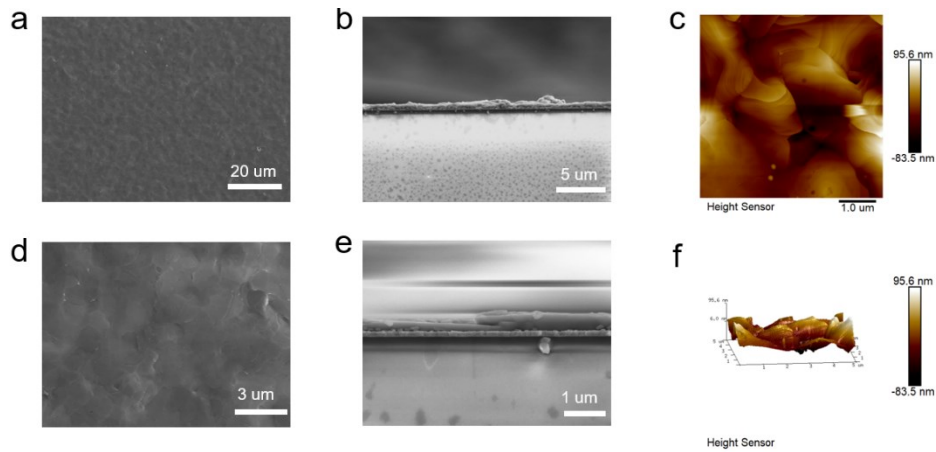


Fig. S11 (a, d) SEM image of the BA_2PbBr_4 polycrystalline film top view with different scale bar. (b, e) Cross-sectional SEM image of BA_2PbBr_4 polycrystalline film with different scale bar. (c, f) AFM image of a BA_2PbBr_4 polycrystalline film surface.

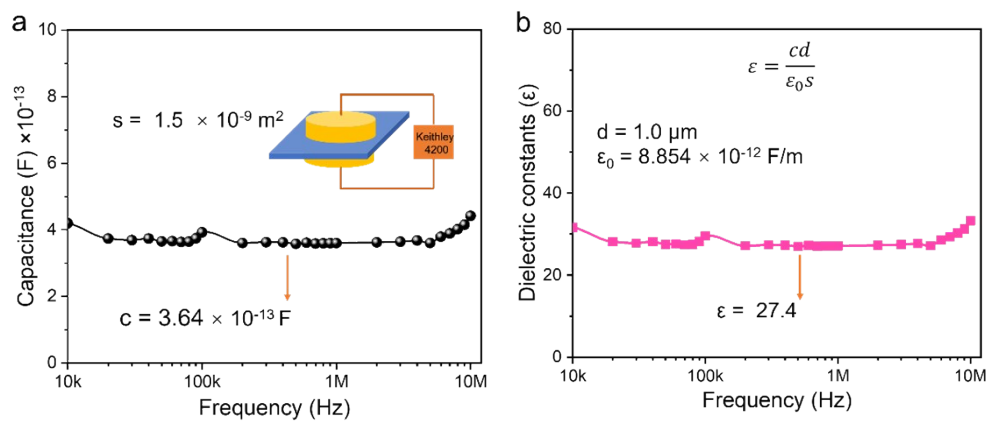


Fig. S12 (a) The capacitance and (b) dielectric constant dependent frequency curves of the BA_2PbBr_4 SCTF. Devices were fabricated by depositing ~ 100 nm thick Au on two opposite surfaces of the BA_2PbBr_4 SCTF. The thickness of the SCTF is $1 \mu\text{m}$. The area is $1.5 \times 10^{-9} \text{m}^2$.

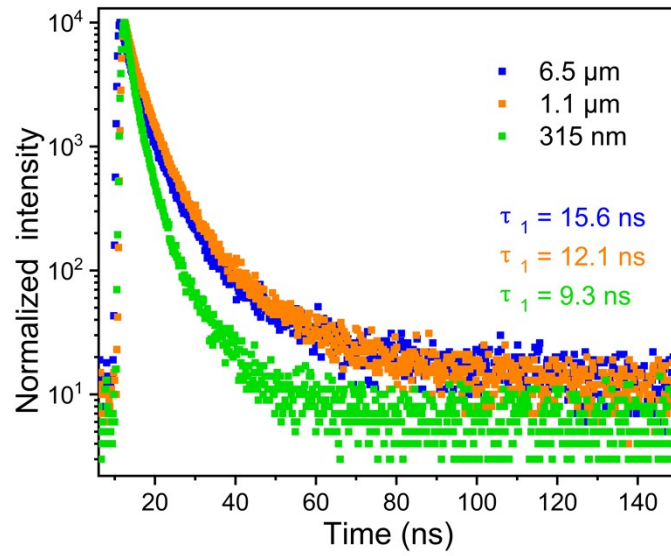


Fig. S13 Time-dependent PL decay curve of BA_2PbBr_4 SCTF with different thickness, the excitation laser beam wavelength is 375 nm.

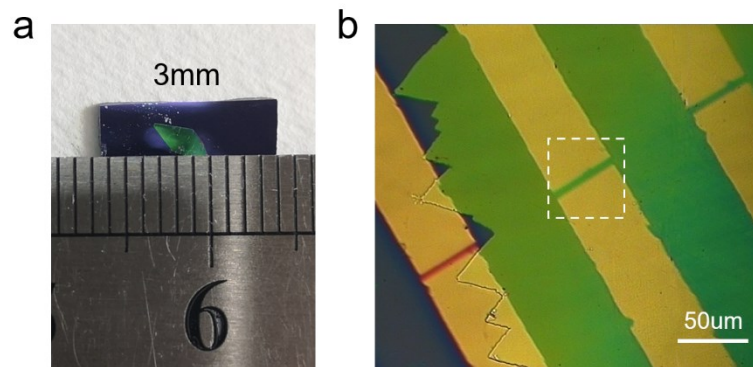


Fig. S14 (a) A photograph of BA_2PbBr_4 SCTF on Si/SiO_2 substrate. (b) The test object illustration of the photosensor.